RSC Advances

PAPER

View Article Online
View Journal | View Issue

Open Access Article. Published on 21 February 2025. Downloaded on 3/25/2026 3:22:57 PM.
This article is licensed under a Creative Commons Attribution-NonCommercial 3.0 Unported Licence.

Check for updates

Cite this: *RSC Adv.*, 2025, **15**, 5906

PX-MDsim: a rapid and efficient platform for large-scale construction of polyamide membranes *via* automated molecular dynamics simulations

Yiran Peng,[a] Chi Zhang,[b] Ming Wu,[a] Guangle Bu,[b] Kai Fan,[a] Xingren Chen,[a] Lijun Liang*[a] and Lin Zhang[bc]

Polyamide (PA) membranes have attracted extensive attention due to their excellent separation performance in water treatment through reverse osmosis and nanofiltration processes. Although numerous molecular simulation studies attempt to explore their advantages from the microstructure, large-scale construction and simulation of PA membranes remain challenging, mainly due to the complexity and computational intensity of cross-linking reactions of polymers in molecular dynamics simulations. This paper introduces an automated platform called PX-MDsim for modeling and simulation of PA membranes. PX-MDsim is based on the PXLink framework and extends its applicability to any monomer with amino ($-NH_2$) and carboxyl ($-COOH$) groups. The platform, combined with the PXLink program, realizes the full-process automated cross-linking simulation from input preparation, initial system construction, force field generation, functional group identification, and charge distribution update. Moreover, the software was used to cross-link *m*-phenylenediamine and 1,4-bis(3-aminopropyl) piperazine with trimesic acid, respectively, and multiple membrane structures with different cross-linking degrees were obtained. Furthermore, the generated membrane microstructure was analyzed using methods such as pore size distribution and order parameter, and the obtained results verified the applicability and accuracy of PX-MDsim in constructing PA membrane structures. The platform is user-friendly and accessible to researchers without prior expertise in molecular dynamics simulation, and it offers new possibilities for polymer research and applications.

Received 22nd December 2024
Accepted 10th February 2025

DOI: 10.1039/d4ra08955c

rsc.li/rsc-advances

1. Introduction

In recent years, polyamide (PA) membranes have become the focus of scientific research due to their outstanding separation performance in water treatment,[1] such as seawater desalination, wastewater recycling, and drinking water purification.[2] Its excellent selectivity and chemical resistance make it a mainstream technology in the water treatment industry, especially in reverse osmosis (RO) and nanofiltration (NF) processes.[3–5]

In the RO process, the PA membrane works by applying high pressure to salt water, causing water molecules to pass through the membrane, while salt and other impurities are retained on the other side of the membrane.[4–6] The NF process is mainly used to separate larger molecules and multivalent ions, and usually operates at lower operating pressures.[1] PA nanofiltration membranes can efficiently separate small molecule organic matter, ions and multivalent metals, and are particularly suitable for water softening, wastewater treatment, and concentration and purification processes in the food and pharmaceutical industries.[7]

At present, there are hundreds of PA membranes formed by cross-linking of different ligands that have been noticed by researchers.[3] One of the most complex and critical steps in simulating PA membranes is modeling. The challenges faced by researchers in large-scale construction of PA membranes mainly stem from the complexity and resource requirements of the polymer cross-linking process.[8] Simulating the cross-linking reaction at the molecular level is not only technically complex, but also is computer consuming.[9,10] There is currently no universal software tool that can flexibly and quickly construct PA membranes based on different monomers and in a personalized manner.

In molecular dynamics (MD) simulations, the construction of PA membranes involves cross-linking reactions of multiple monomer molecules. The cross-linking reaction process is not a simple chemical reaction. It involves non-covalent interactions between molecules, the formation and breaking of chemical bonds, and the accompanying energy and charge changes.[9] After this process, these monomers are finally

[a]College of Automation, Hangzhou Dianzi University, Hangzhou 310018, P.R. China. E-mail: llj@hdu.edu.cn

[b]Engineering Research Center of Membrane and Water Treatment of MOE, College of Chemical and Biological Engineering, Zhejiang University, Hangzhou 310027, P.R. China

[c]Future Environment Laboratory, Innovation Center of Yangtze River Delta, Zhejiang University, Jiaxing 314100, P.R. China

© 2025 The Author(s). Published by the Royal Society of Chemistry

Open Access Article. Published on 21 February 2025. Downloaded on 3/25/2026 3:22:57 PM.
This article is licensed under a Creative Commons Attribution-NonCommercial 3.0 Unported Licence.

connected together through amide bonds to form a highly cross-linked network structure.[11] Therefore, in order to ensure that the structure of the final membrane is consistent with the experimental results, all aspects of this cross-linking process must be accurately handled in the simulation. This requires accurate modeling of force fields, molecular structures, and reaction mechanisms.

Many existing MD simulation software (such as GROMACS, LAMMPS, *etc.*) require users to have an in-depth understanding of each step of the simulation, from force field selection, initial structure generation to the definition of the reaction process, all of which require manual settings by users.[12–15] To simulate cross-linking reactions, users must not only accurately define the chemical reactions in the system but also configure force field parameters for different molecules, which typically requires extensive experience in molecular simulations.[16] For most membrane material researchers, this highly specialized operating threshold greatly limits the popularity and application of the tools. At the same time, existing tools are relatively inefficient when dealing with large-scale simulations. Most tools are not optimized for polymer cross-linking reactions, resulting in slow calculation speeds when dealing with complex molecular systems.[17]

The core function of PXLink is to simulate the cross-linking process of PA membranes, especially to construct polymer networks by calculating the formation of amide bonds between adjacent carboxyl and amino groups. It can effectively generate cross-linked polymer membranes by combining GROMACS for energy minimization and MD simulation. This function has been verified to accurately simulate the structure and dynamic behavior of cross-linked PA membranes of trimesic acid (TMA) and *m*-phenylenediamine (MPD) in water treatment.[9]

PX-MDsim is based on the principle of PXLink and further expands its adaptability so that it is no longer limited to specific monomers. PX-MDsim allows users to simulate cross-linking reaction process between carboxyl and amino groups, enabling to construct various polymer cross-linking systems through amino-carboxyl condensation reaction.

In this paper, we first present the design concept and software framework of PX-MDsim. By automating the steps of input preparation, initial system construction, force field generation, functional group identification, and charge distribution calculation, the repetitive tasks in traditional simulations are simplified, significantly improving simulation efficiency and ease of operation. Furthermore, by simulating the cross-linking reactions of different monomers (*m*-xylylenediamine and TMA, 1,4-bis(3-aminopropyl)piperazine and TMA), and analyzing their properties and structures, the application and reliability of this platform in the construction of polyamide membrane structures are demonstrated, providing a new and efficient tool for the design and optimization of membrane materials.

2. Software description

2.1 Software overview

PX-MDsim is a highly automated MD simulation platform specifically designed to simulate polymer cross-linking reactions with amino ($-NH_2$) and carboxyl (–COOH) monomers, especially suitable for the construction of PA membranes and simulation of the cross-linking process. The software integrates a variety of functional modules and integrates multiple programs such as GROMACS,[12,13] Packmol,[18] CGenff,[19,20] and PXLink.[9] The entire process from input data preparation, force field parameter generation to cross-linking reaction simulation has been automated. PX-MDsim is designed to simplify user operation, reduce human intervention, and significantly increase the efficiency of large-scale simulations.

2.2 Software architecture

2.2.1 Data input and preprocessing. PX-MDsim guides the user to input the necessary monomer information through text prompts, including the structure files and force field files of small molecules with amino and carboxyl groups. The formats of these files include '.pdb', '.mol2' and '.str' files, which contain the spatial structure and force field parameters of the molecules. We recommend using the CGenFF[19,20] platform to easily obtain '.str' files. After that, the software processes these files, generates the initial system according to the user's requirements, and ensures that the input parameters meet the format requirements required for GROMACS simulation. In addition, it is necessary to input the force field file of a molecule in which an amino molecule and a carboxyl molecule are connected by an amide bond. It is used to obtain the bond angle parameters and charge changes at the bonding position after the cross-linking reaction occurs. Before entering these seven files, the user needs to name the file with the residue name of the corresponding molecule. For example, when performing TMA and MPD cross-linking simulations, the '.pdb', '.mol2' and '.str' files of the corresponding molecules are named TMA and MPD, and the force field file of the two molecules connected by amide bonds is named 'TMAMPD.str'.

2.2.2 Force field parameter generation. The software will first extract atomic bonds, angles and other information from the processed '.str' file and append it to the existing residue topology file ('.rtp' file) to ensure that the new molecular structure can be correctly processed in GROMACS. PX-MDsim introduces the cgenff_charmm2gmx script to convert the force field parameters in the CHARMM[21,22] force field file into a format recognizable by GROMACS. The script can automatically parse the molecular structure information in the '.mol2' file, extract the topological information and force field parameters related to the molecule from the .str file, and finally output the GROMACS topology file ('.top' file), which contains all bonds, angles, dihedrals and charge parameters. After that, PX-MDsim will append the new force field parameters to the GROMACS topology file.

2.2.3 Initial system generation. PX-MDsim automatically generates the initial structure of the simulation system by calling Packmol. Packmol is a widely used tool in the early stages of MD simulation. It can arrange the input molecules in a predefined three-dimensional space according to the spatial constraints and number of molecules specified by the user, and ensure that all molecules do not overlap and the spacing

Open Access Article. Published on 21 February 2025. Downloaded on 3/25/2026 3:22:57 PM.
This article is licensed under a Creative Commons Attribution-NonCommercial 3.0 Unported Licence.

between molecules is physically and chemically reasonable, thereby generating a reasonable initial molecular system (Fig. 1).

Afterwards, PX-MDsim uses the 'pdb2gmx' command of GROMACS to generate force field topology information for the entire system. PX-MDsim is pre-configured with the CHARMM36 force field, automatically selects the force field, and calls the 'pdb2gmx' command of GROMACS based on the force field information of the small molecule we added earlier, to match the atoms, bonds, angles and other information in the initial system with the CHARMM36 force field. At the same time, PX-MDsim will automatically prepare an atomic index file for the system according to the residue name.

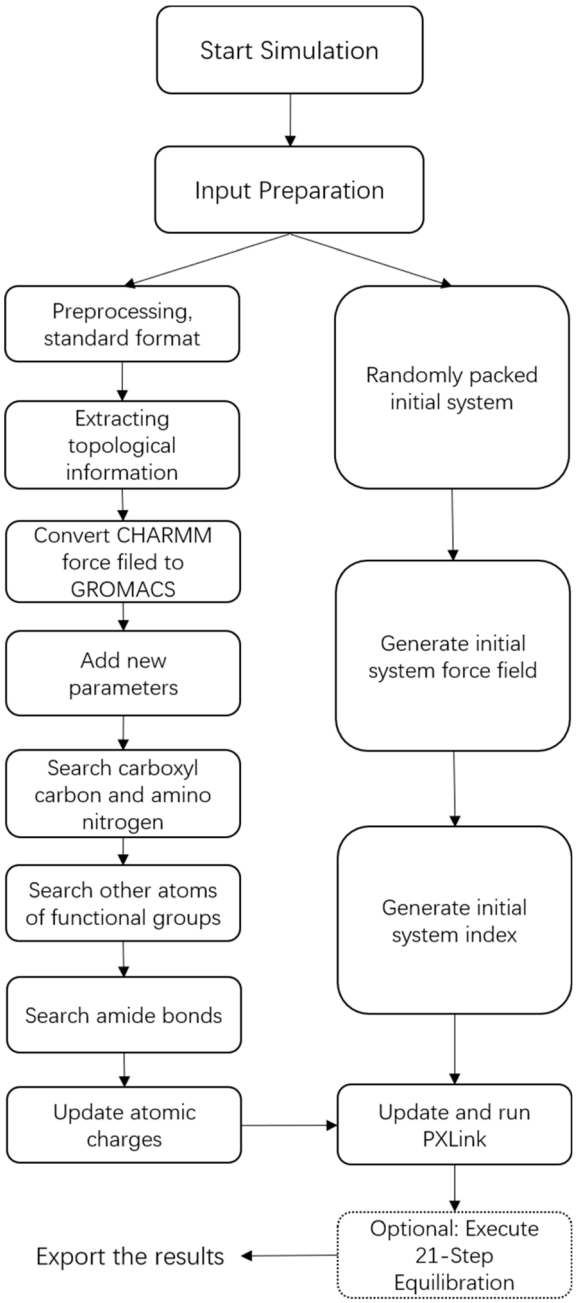

Fig. 1 Flowchart for obtaining the structure of a cross-linked polymer membrane using PX-MDsim. Optional step is marked with dashed boxes.

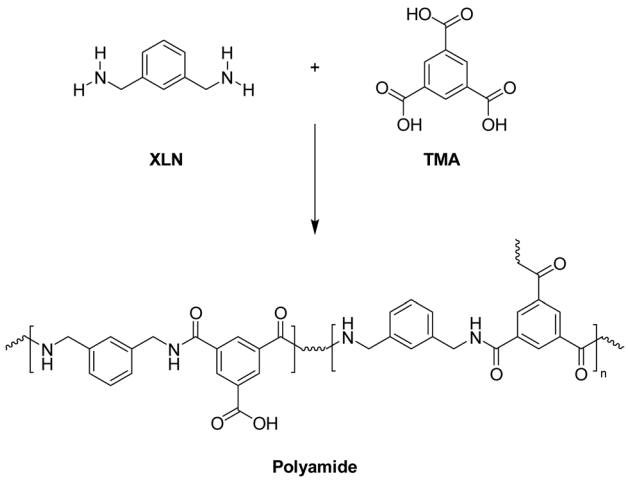

Fig. 2 Structure formula of XLN and TMA monomers and the cross-linked polyamide.

2.2.4 Functional group identification and localization. The essence of a cross-linking reaction is a chemical reaction between two specific functional groups, usually a carboxyl group and an amino group, which form an amide bond through a condensation reaction. By automatically identifying the carboxyl and amino functional groups in the molecule, the software can ensure each cross-linking reaction occurs accurately. At the same time, through this process, PX-MDsim can precisely regulate the degree of crosslinking (DC) of the polymer. The software will sequentially identify the carboxyl and amino functional groups in the molecules uploaded by the user, as well as the amide bond (C–N) in the bimolecular structure. Firstly, the software identifies all atoms of carboxyl functional groups in the molecule. The script parses the bond connection information in the molecule and constructs a connection diagram to record the connection relationship between each atom and other atoms, thereby identifying the carboxyl carbon atom connected to an oxygen atom and a hydroxyl group, and further determines whether the oxygen atom connected to it belongs to the carboxyl oxygen or the hydroxyl oxygen. Secondly, PX-MDsim will identify the nitrogen and hydrogen atoms in the amino group. It also constructs a molecular connection diagram by parsing the bond connection information. After identifying the amino nitrogen atom connected to two hydrogen atoms, the other atoms connected to the amino group are recorded. It ensures that the atom types of all atoms involved in the cross-linking reaction are correctly identified and classified. Finally, PX-MDsim checks the identified carboxyl and amino functional groups to determine whether the oxygen atom connected to the carboxyl carbon atom is also connected to the nitrogen atom in the amino group. By determining the location of the amide bond formation could produce the cross-linking parameters in the subsequent process. The atom types in all identified functional groups will be recorded and replaced in

 © 2025 The Author(s). Published by the Royal Society of Chemistry

Open Access Article. Published on 21 February 2025. Downloaded on 3/25/2026 3:22:57 PM.
This article is licensed under a Creative Commons Attribution-NonCommercial 3.0 Unported Licence.

the PXLink script to ensure that the cross-linking reaction process can be correctly personalized according to the various molecules uploaded by users (Fig. 2).

2.2.5 Update charge distribution. Cross-linking reactions not only involve the formation of chemical bonds, but also lead to change in the charge distribution in the molecular system.[23,24] To ensure that these changes are accurately reflected in the simulation, PX-MDsim automatically updates the charge distribution in the molecular system after each cross-linking reaction. The software can extract the charges of the relevant atoms before and after the reaction, calculate the difference, and then update the corresponding force field file. This step ensures that the molecular structure generated after the cross-linking reaction has a reasonable charge distribution, ensuring the physical and chemical accuracy of the MD simulation results. The software first extracts the atomic charge values related to the crosslinking reaction from the .str file uploaded by the user. Specifically, it reads the charges of the relevant atoms in the newly formed amide bond and the charges of the carboxyl and amino functional group atoms before the reaction. The software automatically finds and returns the charge values of these relevant atoms based on the functional groups and amide bonds identified in the previous step. Next, the script compares the charges of these amide bond atoms extracted with the charge values of the carboxyl and amino functional groups before the reaction and calculates the charge difference between the two. This process extracts the atom types before and after the reaction from different files and determines the charge change through mathematical operations. Finally, the script uses the charge difference as output to update the force field file of the molecular system, ensuring that the new chemical bonds and atomic charges can be accurately described in subsequent MD simulations.

For example, in the cross-linking process of TMA and XLN, the charges of carbonyl carbon, carbonyl oxygen, amide nitrogen, and amide hydrogen after amide bond formation are 0.327, −0.464, −0.416, and 0.313, respectively. Before bonding, the charges of these atoms are 0.456, −0.432, −0.818, and 0.338.

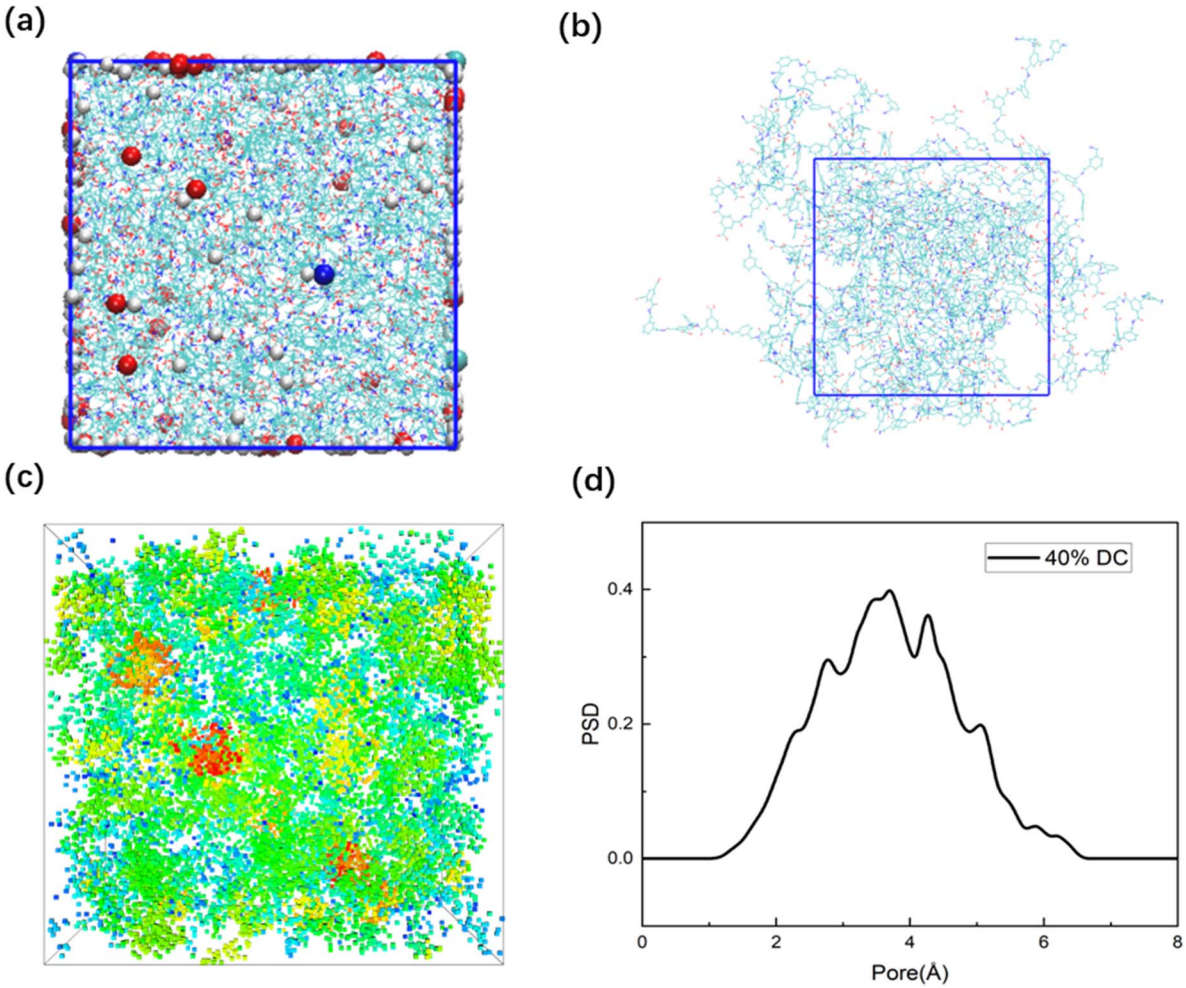

Fig. 3 (a) Snapshot of the initial system. (b) Snapshot of the system with a density of 1.19 g cm^{-3} at 40% DC. (c) Visualization of pore size distribution. Red represents the part with a larger pore size, green represents the part with a medium pore size, and blue represents the part with a smaller pore size. The minimum pore size is 1.1002 Å and the maximum pore size is 6.5 Å. (d) Pore size distribution of cross-linked polymer membranes, the data in the figure are diameters.

Open Access Article. Published on 21 February 2025. Downloaded on 3/25/2026 3:22:57 PM.
This article is licensed under a Creative Commons Attribution-NonCommercial 3.0 Unported Licence.

In addition, the charges of the carbon atoms connected to the carbonyl carbon and amide nitrogen have also changed. Our job is to calculate the charge difference of the relevant atoms before and after bonding, and update its value in the specified function in the PXLink program. In this way, after each new amide bond is formed during the cross-linking process, the correct charge change of the atom will be ensured. The automation of this step ensures the rationality of the charge distribution after the cross-linking reaction, thereby improving the accuracy and credibility of the simulation.

2.2.6 Cross-linking reaction process. We introduced PXLink to perform the simulation of the cross-linking reaction process. PXLink is a Python-based automated script specifically designed to simulate the cross-linking process of polymers such as PA membranes.[9] Its working principle is that through integration with the GROMACS software, the PXLink script can generate chemical bonds between the carboxyl and amino functional groups between molecules to form a three-dimensional cross-linked polymer network. During the cross-linking process, PXLink will identify the functional groups at the reactive sites, determine whether the distance between the two meets the reaction conditions, and determine whether to generate amide bonds based on this. After generating new chemical bonds, the script will perform energy minimization and MD simulations through GROMACS to relax the system and bring it to equilibrium. PXLink will repeat this process until the DC reaches the target value or no more atomic pairs that can form bonds can be found. Finally, PXLink will remove all the remaining molecules in the system that have not been cross-linked, and obtain the cross-linked membrane structure that the user wants.

2.2.7 21-Step compression/relaxation scheme. The 21-step compression/relaxation scheme is a systematic approach employed in molecular simulations to achieve a well-relaxed and stable material structure.[25] This method involves gradually adjusting the system's conditions—typically pressure and volume—through a series of compression and relaxation cycles to allow the material to reach an equilibrium state without sudden energy fluctuations or structural collapse. This scheme is particularly effective for dense materials and those with complex internal networks, such as polymers, where rapid transitions can lead to local minima and artifacts in the simulation results. In PX-MDsim, we have built-in scripts to automatically execute the 21-step compression/relaxation scheme, and users can choose whether to use it as needed. The script uses the GROMACS tool to perform 21 iterations, each time generating a new topology file and running a MD simulation

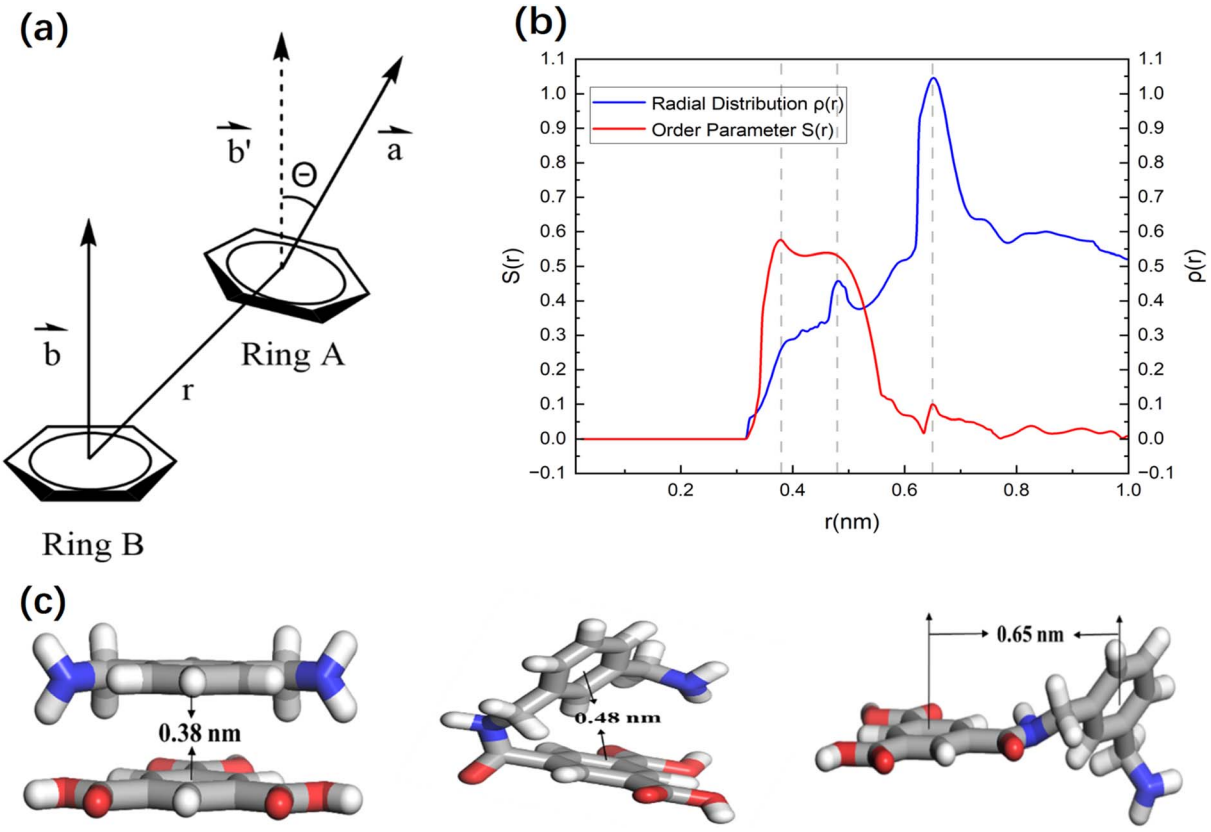

Fig. 4 (a) Schematic representation of the order parameter calculation: r represents the radial distance between the centers of mass of benzene rings, while $\theta(r)$ denotes the angle formed by the normal vectors of adjacent benzene rings at a distance r. (b) The red dashed line is the order parameter $S(r)$ of the adjacent monomers, and the blue solid line is the radial density $\rho(r)$ curve. Based on the distribution of the peaks in the $S(r)$ and $\rho(r)$ spectra and their correlation, three representative structures were identified: $\pi-\pi$ parallel stacking rings at $r \approx 0.38$ nm, T-shaped rings at $r \approx 0.48$ nm, and regular bonding rings at $r \approx 0.65$ nm. (c) Schematic diagram of three benzene ring stacking methods and their corresponding radial distances.

 © 2025 The Author(s). Published by the Royal Society of Chemistry

Open Access Article. Published on 21 February 2025. Downloaded on 3/25/2026 3:22:57 PM.
This article is licensed under a Creative Commons Attribution-NonCommercial 3.0 Unported Licence.

with the corresponding step parameters. The program gradually adjusts the simulation conditions by cyclically calling the 'grompp' and 'mdrun' commands, and checks step by step to ensure that each step runs successfully, and finally reaches a stable equilibrium state of the system. This automated process effectively implements the 21-step simulation and ensures stable and consistent results.

3. Application examples

To evaluate the proposed procedure, simulations were performed using *m*-xylylenediamine (XLN) and trimesic acid (TMA) as well as 1,4-bis(3-aminopropyl)piperazine (DAPP) and TMA as crosslinking monomer inputs to the software. XLN is a versatile crosslinking agent with two reactive amino groups, enabling it to interact with a wide range of acidic or anhydride monomers to form highly crosslinked polymer networks. These crosslinked structures exhibit excellent mechanical strength, chemical resistance, and thermal stability. DAPP is a commonly used crosslinking agent with two amino groups that can react with a variety of acidic or anhydride monomers (such as TMA) to form highly crosslinked polymer membranes. These crosslinked membranes show great potential for application in water treatment, gas separation, and nanofiltration.[26–28] TMA has also been widely studied as a building monomer for crosslinked polymers. Because it contains three carboxyl groups, it can form stable amide bonds with polyamine compounds to construct membrane structures with high mechanical strength and chemical stability.[29,30] Based on its aromatic structure, TMA gives the membrane material high thermal stability and mechanical strength, which makes its application under high temperature and high pressure conditions possible.[31,32] In the field of gas separation, the combination of DAPP and TMA can improve the selectivity for specific gases and optimize industrial separation processes.[27]

In the application cases of XLN and TMA, we mainly selected the membrane structure with a 40% DC to deeply study the internal thin layer structure of the obtained membrane. In the application cases of DAPP and TMA, we obtained four membrane structures with different DC value, respectively, to verify the ability of the program to generate cross-linked polymer membranes with different DC value.

3.1 XLN and TMA

3.1.1 Input file acquisition. The structures of monomer XLN and TMA, as well as the small molecule structure of XLN and TMA connected by an amide bond, were drawn using the advanced molecular editor and visualization tool Gaussview[33] and exported in 'pdb' and 'mol2' formats, respectively. The 'mol2' structure file was uploaded to the CGenFF platform to obtain the force field file in '.str' format.

3.1.2 Initial system creation. Fig. 3(a) shows the initial system we built. The system consists of 305 TMA molecules and 457 XLN molecules randomly stacked in a $5.0 \times 5.0 \times 7.0$ nm^3 cube with an initial density of 1.19 g cm^{-3} and a 1 : 1 ratio of free carboxyl and amine groups. The process is automated and the user only needs to input the necessary parameters.

3.1.3 Results and analysis. By modifying the target DC value, a membrane system with a 40% DC and unreacted irrelevant parts removed was obtained. The resulting membrane structure is shown in Fig. 3(b). We then calculated the pore size distribution (PSD) of the cross-linked polymer membrane using zeo++.[34–36] Fig. 3(c) shows the three-dimensional spatial distribution of the pore size in the membrane, with the color gradient from blue to red corresponding to the change in pore size from small to large. The minimum pore size is 1.1002 Å and the maximum pore size is 6.5 Å. As seen in Fig. 3(c), the large pore parts (red part) is not evenly distributed, but is mainly concentrated in the local hot spot area, showing a certain aggregation. These areas may correspond to the parts of the membrane material with a low DC value. The small pore parts (blue and green parts) are more evenly distributed, covering the main structure of the membrane, which shows that the overall structure of the membrane has a certain regularity.

It can be seen from the Fig. 3(d), PSD from the simulation results exhibits a normal distribution. The main peak value of pore size ranges between 3 Å and 5 Å, corresponding to the green and yellow parts in Fig. 3(c). It is consistent with the PSD of the nanofiltration membrane from the experiment,[37–40] verifying the accuracy of the membrane structure obtained by the program. In addition, secondary peaks are observed in both the small pore size area (<3 Å) and the larger pore size area (>5 Å). The distribution of small pore regions may be related to the close packing

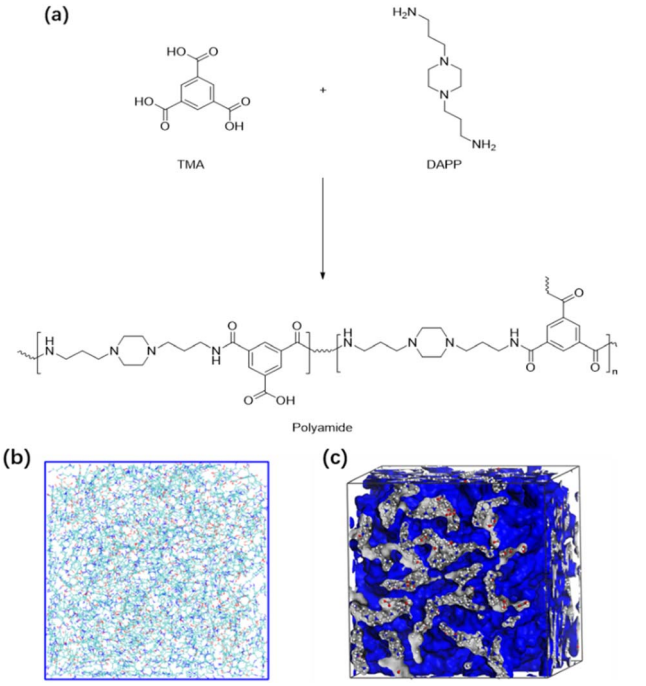

Fig. 5 (a) Structure formula of DAPP and TMA monomers and the crosslinked polyamide. (b) Snapshot of the initial system. (c) 3D pore distribution map. The box size is 6.0 × 6.0 × 6.0 nm3 and the density is 0.8 g cm^{-3}.

Open Access Article. Published on 21 February 2025. Downloaded on 3/25/2026 3:22:57 PM.
This article is licensed under a Creative Commons Attribution-NonCommercial 3.0 Unported Licence.

of polymer segments, while the distribution of large pore regions may be caused by insufficient local cross-linking.

In addition to this, the order parameter $S(r)$ and radial density $\rho(r)$ were evaluated to more accurately investigate the local structure within the cross-linked thin layer, which is mainly controlled by the interactions between the phenyl groups of the bonded and non-bonded monomers.[41] Fig. 4 explains the calculation basis of these parameters. Here, r denotes the radial distance between the centers of mass of the phenyl rings, while $\theta(r)$ refers to the angle formed by the normal vectors of neighboring phenyl rings at a distance r. The order parameter $S(r)$ is expressed mathematically as

$$S(r) = \frac{3\cos^2(\theta(r)) - 1}{2} \tag{1}$$

In this context, $S(r) = 0$ indicates a random arrangement, whereas $S(r) = 1$ signifies a perfectly ordered packing. The relative local density of benzene rings, $\rho(r)$, is calculated using the equation

$$\rho_r = \frac{\rho(r)}{\rho_{\text{bulk}}} \tag{2}$$

where $\rho(r)$ represents the density of benzene rings at a distance r, and the bulk density ρ_{bulk} is defined for $r > 1$ nm.

As shown in Fig. 4(b), the order parameter $S(r)$ exhibits a sharp peak at $r \approx 0.38$ nm, corresponding to the π–π stacking structure, while a smaller peak appears at $r \approx 0.65$ nm, attributed to regularly bonded benzene rings. On the other hand, the radial density distribution $\rho(r)$ reveals a significant peak at $r \approx 0.65$ nm, which corresponds to the distribution of $S(r)$. This prominent peak in $\rho(r)$ suggests that the majority of local structures in the cross-linked polymer film thin layer are covalently bonded rings with slightly twisted orientations. Additionally, another peak observed at $r \approx 0.48$ nm corresponds to T-shaped rings, indicating a higher occurrence of bent structures in the thin layer. These structural differences may result in larger pore sizes compared to the ordered π–π stacking structures. These results are basically consistent with the study of order function in other cross-linked polyamide membranes, and also verify the rationality of the membrane structure obtained by our procedure.

The position $r \approx 0.38$ nm corresponds to the parallel π–π stacking between benzene rings. At this distance, the molecules

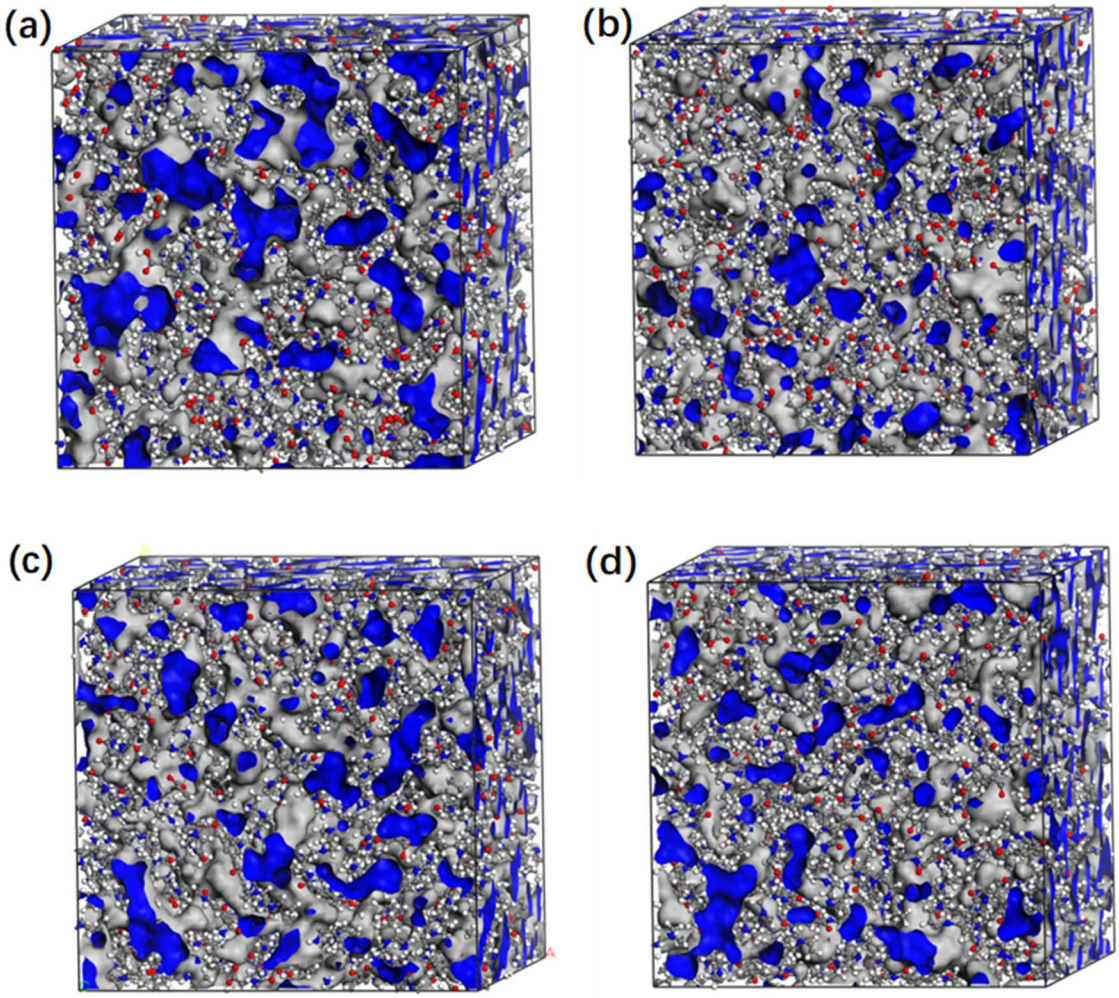

Fig. 6 Pore distribution map of four polymer membranes with DC: (a) 20%; (b) 40%; (c) 60% and (d) 80%, respectively. The grey areas represent the occupied space and the blue areas represent the free volume.

 © 2025 The Author(s). Published by the Royal Society of Chemistry

Open Access Article. Published on 21 February 2025. Downloaded on 3/25/2026 3:22:57 PM.
This article is licensed under a Creative Commons Attribution-NonCommercial 3.0 Unported Licence.

tend to be arranged in a regular and orderly manner, and $S(r)$ shows a significant peak. Although there are two geometric stacking modes at $r \approx 0.48$ nm and $r \approx 0.65$ nm, there may be a certain degree of rotational freedom between the benzene rings in these two stacking modes. Different from the π–π stacking, the molecules in these two models are in a relatively free or random orientation state, and it reduces the $S(r)$ value.

3.2 DAPP and TMA

3.2.1 Input file acquisition. Similar to the method in the previous example, the structures of monomer DAPP and TMA, as well as the small molecule structure of DAPP and TMA connected by an amide bond, were drawn using the advanced molecular editor and visualization tool Gaussview[33] and exported in 'pdb' and 'mol2' formats, respectively. The 'mol2' structure file was uploaded to the CGenFF platform to obtain the force field file in '.str' format.

3.2.2 Initial system creation. As seen in Fig. 5(b and c), the initial system consists of 200 TMA molecules and 300 DAPP molecules randomly stacked in a $6.0 \times 6.0 \times 6.0$ nm^3 cube with an initial density of 0.8 g cm^{-3} and a 1 : 1 ratio of free carboxyl and amine groups.

3.2.3 Results and analysis. By modifying the target DC values, we obtained membrane systems with different DC varied from 20%, 40%, 60% to 80%. Fig. 6 shows the visualized pore size distribution of the four polymer membranes. The grey areas represent the occupied space, while the blue parts represent the free volume. It can be seen from the figure that the membrane pores are distributed relatively uniformly in all four systems. They were then divided into two groups, one group used the 21-step equilibrium method on the obtained membrane structures, and the other group performed hydration simulation on the membrane structures. The PSD of the two groups of cross-linked membrane systems were calculated using the zeo++[34–36] tool, and the PSD diagrams of each cross-linked membrane were obtained, as shown in Fig. 7 and 8. Fig. 7 shows the PSD of the membrane structure after 21-step equilibrium method. It can be seen that most of the pore sizes are around 0.4 nm, with peak values of 4.1 Å, 3.8 Å, 4.2 Å, and 4.2 Å, respectively. The PSD did not show significant differences with the change of DC. It indicates that the 21-step equilibrium method can stabilize the micro-structural properties of the membrane under different DC conditions, providing a reliable modeling method and experimental basis for subsequent research.

Fig. 8 shows the PSD of the hydrated membranes. Membranes with low DC usually have more structural irregularities, resulting in larger holes or aggregate pores, which show a wider PSD. As the DC increases, more covalent bonds are formed, resulting in a denser membrane structure. This reduces

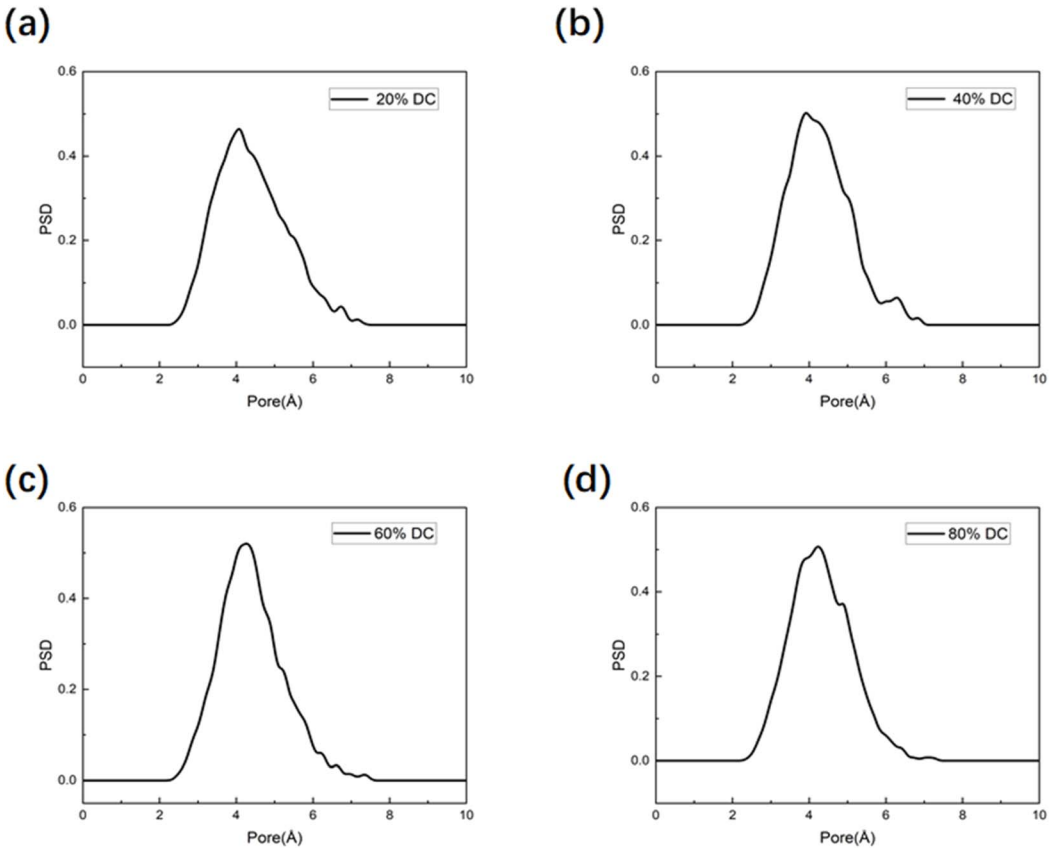

Fig. 7 The PSD data of the four polymer membranes were obtained using the 21-step equilibrium method with DC: (a) 20%; (b) 40%; (c) 60% and (d) 80%, respectively, with peak values correspond to pore sizes of 4.1 Å, 3.8 Å, 4.2 Å, and 4.2 Å, respectively. The data observed in the figure are all normally distributed.

Open Access Article. Published on 21 February 2025. Downloaded on 3/25/2026 3:22:57 PM.
This article is licensed under a Creative Commons Attribution-NonCommercial 3.0 Unported Licence.

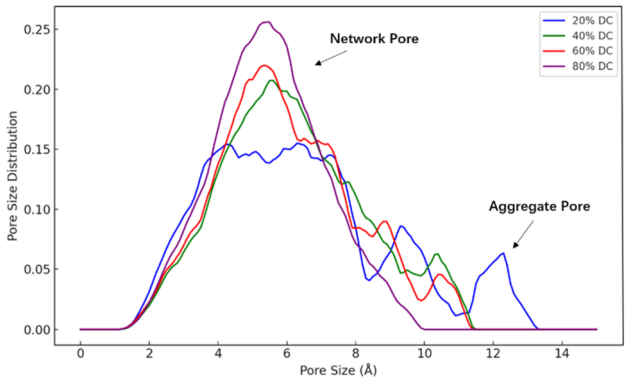

Fig. 8 PSD of the solvated membranes formed by DAPP and TMA with different DC. Aggregate pores are larger pores formed by loose packing or incompletely cross-linked regions between polymer chains. Network pores are small, uniform pores formed by a highly cross-linked network of polymer chains.

the free volume within the membranes, effectively reducing the pore size. Therefore, the PSD becomes more concentrated and the pore size decreases. These findings are in strong agreement with the results reported in related study.[42]

All the PSD of different membranes exhibit a normal distribution. It is in consistent with the experimental results. The pore diameter of a general nanofiltration membrane is usually between 0.1 nm and 1 nm (ref. 37–40) from the experiment, which is in good agreement with the PSD of the nanofiltration membrane in our simulation. At the same time, in another simulation of a typical polyamide membrane, the researchers measured the pore diameter of the dry membrane made of MPD and TMA to be 0.4 nm,[9] which is consistent with the pore size data measured in this case. It confirms that the PX-MDsim is suitable for building the nanofiltration membrane by amino-carboxyl condensation reaction.

4. Conclusions

In this study, PX-MDsim is proposed, an innovative MD simulation platform designed for the construction and simulation of PA membranes *via* automated cross-linking amino-carboxyl condensation reaction. PX-MDsim effectively extends the functionality of PXLink, providing greater flexibility in simulating a variety of monomers containing amino and carboxyl groups. This paper introduces two application examples in detail. The rationality and reliability of the membrane structure obtained by the software platform were verified by analyzing the order parameters and pore size distribution of the PA membrane obtained by crosslinking XLN and TMA. The flexibility and efficiency of the platform in constructing PA membranes with different DC values were highlighted by simulating the cross-linking process of DAPP and TMA and verifying the pore size distribution of the results.

In future work, we plan to further optimize the algorithm of PX-MDsim to accelerate the computation and improve the accuracy of force field parameter generation. It is worth emphasizing that PX-MDsim not only provides an efficient simulation method for current polymer research and membrane material design, but more importantly, it can easily generate a large amount of simulation data. These large-scale data create conditions for the application of machine learning and artificial intelligence in the design of new materials. By leveraging the diverse datasets generated by PX-MDsim, we hope to lay the foundation for AI-driven materials science research in the future, thereby promoting the process of automated and intelligent materials development. This prospect will enable PX-MDsim to play an even more important role in the modern technology of new material design and optimization.

This software is free and open to everyone. For specific usage methods, please refer to the software documentation in the repository.

Data availability

PX-MDsim is a free software and open to everyone. Installation instructions, source code, latest documentation, and example usage can be accessed on the GitHub repository (**https://github.com/AI4SCI-HDU**).

Author contributions

Yiran Peng: investigation, data curation, writing – original draft. Chi Zhang: investigation, data curation. Guangle Bu: data curation. Kai Fan: conceptualization, data curation. Xingren Chen: methodology. Ming Wu: investigation, data curation. Lin Zhang: conceptualization, methodology, writing– review & editing. Lijun Liang: conceptualization, methodology, supervision, resources, writing – review & editing.

Conflicts of interest

There are no conflicts of interest to declare.

Acknowledgements

This work was financially supported by National Natural Science Foundation of China (22276045, 22138010); Joint R&D of the Yangtze River Delta Science and Technology Innovation Community (2023CSJGG1000); Key R&D project of Anhui Province (No. 202304a05020022). We would like to thank Xiang Huang from Shaoxing Testing Institute of Quality and Technical Supervision, Shaoxing 312000, China for assisting with processing data during manuscript revisions.

References

1 P. Sarkar, C. Wu, Z. Yang and C. Y. Tang, *Chem. Soc. Rev.*, 2024, **53**, 4374–4399.
2 J. Usman, S. I. Abba, F. J. Abdu, L. T. Yogarathinam, A. G. Usman, D. Lawal, B. Salhi and I. H. Aljundi, *RSC Adv.*, 2024, **14**, 31259–31273.
3 M. A. Ahmed, S. A. Mahmoud and A. A. Mohamed, *RSC Adv.*, 2024, **14**, 18879–18906.

 © 2025 The Author(s). Published by the Royal Society of Chemistry

Open Access Article. Published on 21 February 2025. Downloaded on 3/25/2026 3:22:57 PM.
This article is licensed under a Creative Commons Attribution-NonCommercial 3.0 Unported Licence.

4 T. R. Nickerson, E. N. Antonio, D. P. McNally, M. F. Toney, C. Ban and A. P. Straub, *Chem. Sci.*, 2023, **14**, 751–770.
5 W. Liu, J. L. Livingston, L. Wang, Z. Wang, M. del Cerro, S. A. Younssi, R. Epsztein, M. Elimelech and S. Lin, *Nat. Rev. Methods Primers*, 2024, **4**, 10.
6 H. Takabatake, M. Taniguchi and M. Kurihara, *Membranes*, 2021, **11**, 138.
7 M. Peydayesh, *Membranes*, 2022, **12**, 518.
8 M. Q. Seah, W. J. Lau, P. S. Goh, H.-H. Tseng, R. A. Wahab and A. F. Ismail, *Polymers*, 2020, **12**, 2817.
9 C. Zhang, G. Bu, M. S. J. Sajib, L. Meng, S. Xu, S. Zheng, L. Zhang and T. Wei, *Comput. Phys. Commun.*, 2023, **291**, 108840.
10 K. Li, S. Li, L. Liu, W. Huang, Y. Wang, C. Yu and Y. Zhou, *Phys. Chem. Chem. Phys.*, 2019, **21**, 19995–20002.
11 Y. Li, M. Wang, L. Wang, T. Chen, W. Feng, T. Wang and L. Zhao, *Phys. Chem. Chem. Phys.*, 2023, **25**, 25309–25321.
12 H. J. C. Berendsen, D. van der Spoel and R. van Drunen, *Comput. Phys. Commun.*, 1995, **91**, 43–56.
13 B. Hess, C. Kutzner, D. van der Spoel and E. Lindahl, *J. Chem. Theory Comput.*, 2008, **4**, 435–447.
14 S. Plimpton, *J. Comput. Phys.*, 1995, **117**, 1–19.
15 A. P. Thompson, H. M. Aktulga, R. Berger, D. S. Bolintineanu, W. M. Brown, P. S. Crozier and R. Shan, *Comput. Phys. Commun.*, 2022, **271**, 108171.
16 S. Duangdangchote, D. S. Seferos and O. Voznyy, *Digital Discovery*, 2024, **3**, 2177–2182.
17 A. V. Karatrantos, O. Couture, C. Hesse and D. F. Schmidt, *Polymers*, 2024, **16**, 1373.
18 L. Martínez, R. Andrade, E. G. Birgin and J. M. Martínez, *J. Comput. Chem.*, 2009, **30**, 2157–2164.
19 K. Vanommeslaeghe, E. Hatcher, C. Acharya, S. Kundu, S. Zhong, J. Shim, E. Darian, O. Guvench, P. Lopes, I. Vorobyov and A. D. Mackerell Jr, *J. Comput. Chem.*, 2010, **31**, 671–690.
20 K. Vanommeslaeghe, E. P. Raman and A. D. Mackerell Jr, *J. Chem. Inf. Model.*, 2012, **52**, 3144–3154.
21 A. D. Mackerell Jr, D. Bashford, M. Bellott, R. L. Dunbrack Jr, J. D. Evanseck, M. J. Field, S. Fischer, J. Gao, H. Guo, S. Ha, D. Joseph-McCarthy, L. Kuchnir, K. Kuczera, F. T. K. Lau, C. Mattos, S. Michnick, D. T. Nguyen, B. Prodhom, W. E. Reiher III, B. Roux, M. Schlenkrich, J. C. Smith, R. Stote, J. Straub, M. Watanabe, J. Wiorkiewicz-Kuczera, D. Yin and M. Karplus, *J. Phys. Chem. B*, 1998, **102**, 3586–3616.
22 J. B. Klauda, R. M. Venable, J. A. Freites, J. W. O'Connor, D. J. Tobias, C. Mondragon-Ramirez, I. Vorobyov, A. D. Mackerell Jr and R. W. Pastor, *J. Phys. Chem. B*, 2010, **114**, 7830–7843.
23 J. Cheng, H. Wang, Y. Zhang, X. Wang and G. Liu, *Org. Biomol. Chem.*, 2024, **22**, 7549–7559.
24 J. Kang, C. Wang, D. Li, G. He and H. Tan, *Phys. Chem. Chem. Phys.*, 2015, **17**, 16519–16524.
25 G. S. Larsen, P. Lin, K. E. Hart and C. M. Colina, *Macromolecules*, 2011, **44**, 6944–6951.
26 K. A. Veetil, S. Kannan, E. K. Sun, M. H. Kabir, O. Choi, I. Hossain and T.-H. Kim, *Sep. Purif. Technol.*, 2025, **359**, 130755.
27 Y. Oya, M. Nakazawa, K. Shirasu, Y. Hino, K. Inuyama, G. Kikugawa, J. Li, R. Kuwahara, N. Kishimoto, H. Waizumi, M. Nishikawa, A. Waas, N. Odagiri, A. Koyanagi, M. Salviato and T. Okabe, *Chem. Phys. Lett.*, 2021, **762**, 138104.
28 M. S. Ragab, M. R. Shehata, M. M. Shoukry, M. Haukka and M. A. Ragheb, *RSC Adv.*, 2022, **12**, 1871–1884.
29 J. Smith, R. Wang and T. Liu, *Polym. Chem.*, 2023, **14**, 1456–1473.
30 X. Li, Y. Zhao and L. Chen, *J. Polym. Res.*, 2023, **30**, 45001.
31 J. A. Reglero Ruiz, M. Trigo-López, F. C. García and J. M. García, *Polymers*, 2017, **9**, 414.
32 D. Rana and T. Matsuura, *Environ. Sci.:Water Res. Technol.*, 2015, **1**, 431–459.
33 M. J. Frisch, G. W. Trucks, H. B. Schlegel, G. E. Scuseria, M. A. Robb, J. R. Cheeseman, *et al.*, *Gaussian 16, Revision C.01*, Gaussian, Inc., Wallingford CT, 2016.
34 T. F. Willems, C. H. Rycroft, M. Kazi, J. C. Meza and M. Haranczyk, *Microporous Mesoporous Mater.*, 2012, **149**, 134–141.
35 M. Pinheiro, R. L. Martin, C. H. Rycroft, A. Jones, E. Iglesia and M. Haranczyk, *J. Mol. Graphics Modell.*, 2013, **44**, 208–219.
36 D. Ongari, P. G. Boyd, S. Barthel, M. Witman, M. Haranczyk and B. Smit, *Langmuir*, 2017, **33**(51), 14529–14538.
37 C. D. Roth, S. C. Poh and D. X. Vuong, *Nanotechnology Applications for Clean Water*, 2nd edn, 2014, pp. 201–207.
38 Y. Chen, C. Shen and F. Fang, *Desalination*, 2020, **494**, 114640.
39 Y. H. Teow, J. Y. Sum, K. C. Ho and A. W. Mohammad, *Osmosis Eng.*, 2021, 53–95.
40 D. J. Johnson and N. Hilal, *Desalination*, 2022, **524**, 115480.
41 T. Wei, L. Zhang, H. Zhao, H. Ma, M. S. J. Sajib, H. Jiang and S. Murad, *J. Phys. Chem. B*, 2016, **120**, 10311–10318.
42 J. He, J. Yang, J. R. McCutcheon and Y. Li, *J. Membr. Sci.*, 2022, **658**, 120731.

© 2025 The Author(s). Published by the Royal Society of Chemistry